Applied Mathematical Sciences, Vol. 11, 2017, no. 7, 299 - 309
HIKARI Ltd, www.m-hikari.com
https://doi.org/10.12988/ams.2017.64155

Analysis of Signal to Noise Ratio on Restored Multispectral Data

Asmala Ahmad

Department of Industrial Computing
Faculty of Information and Communication Technology
Universiti Teknikal Malaysia Melaka
Melaka, Malaysia

Shaun Quegan

Department of Applied Mathematics
School of Mathematics and Statistics
University of Sheffield
Sheffield, United Kingdom

Abstract

An analysis of signal to noise ratio (SNR) of restored multispectral data is reported. The data comes from multispectral satellite sensor and has undergone a restoration process due to the degradation by atmospheric haze. The restoration involves subtracting haze mean due to haze scattering and filtering haze randomness due to haze spatial variability. The results shows that the SNR of restored data after Gaussian filtering is higher than average and median filtering. The improvement of SNR at short and moderate visibilities is more significant than good visibilities.

Keywords: SNR, Haze, Visibility, Landsat, Filtering

1 Introduction

In [8], we developed a model for hazy satellite data, which can be expressed as:

$$L_i(V) = \left(1 - \beta_i^{(1)}(V)\right) T_i + L_O + \beta_i^{(2)}(V) H_i \tag{1}$$

where $L_i(V)$, T_i, H_i, L_o, $\beta_i^{(1)}$ and $\beta_i^{(2)}$ are the hazy dataset, the signal component, the pure haze component, the radiance scattered by the atmosphere, the signal attenuation factor and the haze weighting in satellite band i, respectively. H_i can be expressed as:

$$H_i = \overline{H_i} + H_{i_v} \tag{2}$$

Where $\overline{H_i}$ is the haze mean, which is assumed to be uniform within the image or sub-region of the image, and H_{i_v} is a zero-mean random variable corresponding to haze randomness. Hence:

$$\mathrm{Var}\left(H_{i_v}\right) = \mathrm{Var}\left(H_i\right) \tag{3}$$

So Equation (1) can be written as:

$$L_i(V) = \left[1 - \beta_i^{(1)}(V)\right] T_i + L_O + \beta_i^{(2)}(V)\left[\overline{H_i} + H_{i_v}\right] \tag{4}$$

In order to remove the haze effects [4], [5], [10] we need to remove both the weighted haze mean $\beta_i^{(2)}(V)\overline{H_i}$ and the varying component $\beta_i^{(2)}(V)H_{i_v}$ and deal with the signal attenuation factor $\beta_i^{(1)}(V)$. The effects of $\beta_i^{(1)}(V)$ to classification accuracy are not significant [8], so we will not consider their removal throughout the analysis. We normally do not have prior knowledge about $\beta_i^{(2)}(V)\overline{H_i}$ therefore we need to estimate it from the hazy data itself. If the estimate is $\widehat{\beta_i^{(2)}(V)\overline{H_i}}$, subtracting it from $L_i(V)$ yields:

$$\widehat{L_{i_Z}(V)} = L_i(V) - \widehat{\beta_i^{(2)}(V)\overline{H_i}} = \left[1 - \beta_i^{(1)}(V)\right] T_i + L_O + \beta_i^{(2)}(V)\left[\overline{H_i} + H_{i_v}\right] - \widehat{\beta_i^{(2)}(V)\overline{H_i}} \tag{5}$$

Equation (5) becomes:

$$\widehat{L_{i_Z}(V)} = \left[1 - \beta_i^{(1)}(V)\right] T_i + \left[\beta_i^{(2)}(V)\overline{H_i} - \widehat{\beta_i^{(2)}(V)\overline{H_i}}\right] + \beta_i^{(2)}(V)H_{i_v} + L_O \tag{6}$$

where $\left[\beta_i^{(2)}(V)\overline{H_i} - \widehat{\beta_i^{(2)}(V)\overline{H_i}}\right]$ is the error associated with the difference between the ideal and estimated weighted haze mean. A common way to measure the accuracy of restored data is to compare its quality with uncorrupted data. Visual analysis offers a fast and simple way to do this, but suffers from possible analyst

bias. Hence we propose two quantitative approaches to assess the quality of restored data. Note that here we assume $\left[1-\beta_i^{(1)}(V)\right]T_i$ from the hazy data to be the signal amplitude because the effects of $\left[1-\beta_i^{(1)}(V)\right]$ to data quality is negligible; this applies for all cases. Due to the discrete properties of the hazy data, the exact values are replaced by their estimates:

$$\widehat{SNR} = \frac{\sum_{m=1}^{Q_m}\sum_{n=1}^{Q_n}\left\{\left[1-\beta_i^{(1)}(V)\right]T_i + L_O\right\}^2}{\sum_{m=1}^{Q_m}\sum_{n=1}^{Q_n}\beta_i^{(2)}(V)^2\left(\overline{H}_i + H_{i_v}\right)^2} \tag{7}$$

where Q_m and Q_n are the numbers of pixels in the rows and columns of the image respectively. Note that such calculation is only possible if the values of T_i, $\overline{H}_i$, H_{i_v}, $\beta_i^{(1)}(V)$, $\beta_i^{(2)}(V)$, Q_m and Q_n are known a priori. Hence the SNR after subtraction of the haze mean is:

$$\widehat{SNR} = \frac{\sum_{m=1}^{Q_m}\sum_{n=1}^{Q_n}\left\{\left[1-\beta_i^{(1)}(V)\right]T_i + L_O\right\}^2}{\sum_{m=1}^{Q_m}\sum_{n=1}^{Q_n}\beta_i^{(2)}(V)^2 H_{i_v}{}^2} \tag{8}$$

For linear filtering we have:

$$\widehat{SNR} = \frac{\sum_{m=1}^{Q_m}\sum_{n=1}^{Q_n}\left\{\left[1-\beta_i^{(1)}(V)\right]T_i + L_O\right\}^2}{\sum_{m=1}^{Q_m}\sum_{n=1}^{Q_n}\left\{\left[1-\beta_i^{(1)}(V)\right]\left[h_{linear}(T_i) - T_i\right] + \beta_i^{(2)}(V)h_{linear}\left(H_{i_v}\right)\right\}^2} \tag{9}$$

For median filtering we have:

$$\widehat{SNR} = \frac{\sum_{m=1}^{Q_m}\sum_{n=1}^{Q_n}\left\{\left[1-\beta_i^{(1)}(V)\right]T_i + L_O\right\}^2}{\sum_{m=1}^{Q_m}\sum_{n=1}^{Q_n}\left\{\begin{array}{l}\text{Median}\left(\left[1-\beta_i^{(1)}(V)\right]T_i + \beta_i^{(2)}(V)H_{i_v} + L_O\right) - \\ \left[1-\beta_i^{(1)}(V)\right]T_i - L_O\end{array}\right\}^2} \tag{10}$$

2 Calculation of SNR

In this section, we calculate the SNR of the data after weighted mean subtraction and filtering for the case when the haze mean is known exactly. The SNR calculations for bands 1 are given first and the explanation is given after that. These are then followed by the SNR calculations for bands 2, 3, 4, 5 and 7. This makes use of the simulated dataset for visibilities 2 km to 18 km. Figure 1 shows the SNR for band 1 with the exact mean removed, after applying average, median and Gaussian filtering. These plots help to determine the window size that produces the highest SNR at a particular visibility.

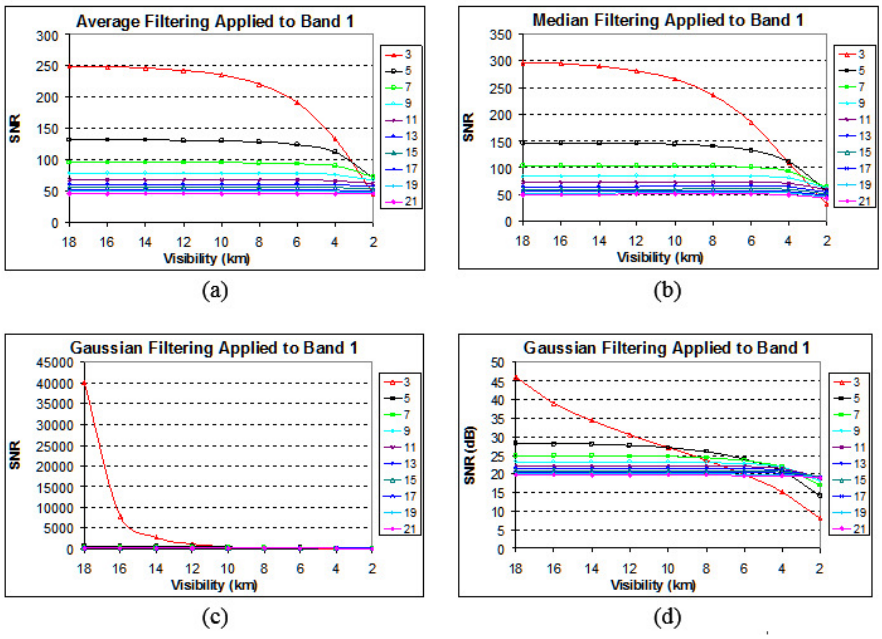

Figure 1: SNR for band 1 after applying (a) average filtering, (b) median filtering, (c) Gaussian filtering and (d) Same as (c) but in dB.

For average and median filtering (Figure 1 (a and b)), for smaller window sizes, the drop in SNR gets more rapid as the visibility reduces, but for bigger sizes, the SNR is nearly constant for all visibilities. For longer and moderate visibilities, 3 x 3 windows give the highest SNR, but the SNR drops when the window size is increased. For very short visibilities, bigger windows produce higher SNRs. For Gaussian filtering (Figure 1 (c)), the 3 x 3 window shows a sharp decrease in SNR for long visibilities, but then a slow decline for moderate visibilities. A big difference in SNR is observed between the 3 x 3 window and the rest of the windows, particularly for long visibilities. The larger-sized windows show a relatively flat trend towards shorter visibilities. The separation of the effect of window sizes is much better in the dB plot (Figure 1 (d)). It can be seen that, for longer visibilities, smaller windows show higher SNR than bigger windows, while

for shorter visibilities, the bigger windows exhibit higher SNRs, but the separation between windows is relatively narrow.

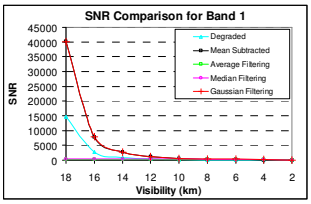

(a)

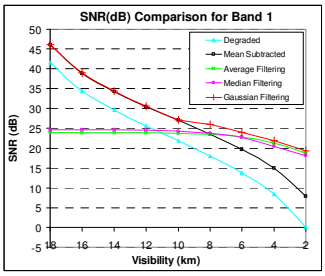

(b)

Figure 2: Comparison of filter performances for band 1.

Table 1: Optimal window sizes for band 1.

Visibility (km)	Filter Types / Sizes		
	Average	Median	Gaussian
2	7	7	15
4	3	5	7
6	3	3	5
8	3	3	5
10	3	3	3
12	3	3	3
14	3	3	3
16	3	3	3
18	3	3	3

For all types of filtering, the highest SNR for a particular visibility (associated with the corresponding optimal window size in Table 1) is plotted in Figure 2(a). The SNR for Gaussian filtered data is very close to weighted-mean subtracted data and noticeably improves the original degraded data at shorter visibilities. The dB plot in Figure 2(b) provides a better separation for all types of filtering, where Gaussian filtering shows the best SNR for all visibilities. The changes in trend in the middle of the Gaussian filtering curve is due to a transition of the corresponding window sizes, i.e. the window size changes from 3 x 3 (at 10 km visibility) to 5 x 5 (at 8 km visibility). The improvement made by the Gaussian filtering with respect to weighted-mean subtracted data and degraded data curves is likely to increase as visibility reduces. The average and median filtering show a lower SNR than the degraded and weighted-mean subtracted data, for longer visibilities, indicating that the quality of the data becomes poorer after filtering compared to before filtering. However, the SNR of the average-filtered and the median-filtered data is better than the degraded and mean subtracted data for shorter visibilities.

3 Explanation of the SNR Results

In order for the filtered data to have higher SNR than the mean subtracted data, the denominator in Equations (9) and (10) should be smaller than that of (8). From (8) and (9), the denominator difference is:

$$\sum_{m=1}^{Q_m}\sum_{n=1}^{Q_n}\left\{\left[\beta_i^{(2)}(V)\right]^2 H_{i_v}{}^2-\left\{\left(1-\beta_i^{(1)}(V)\right)\left[h_{linear}(T_i)-T_i\right]+\beta_i^{(2)}(V)h_{linear}\left(H_{i_v}\right)\right\}^2\right\}$$

$$=\sum_{m=1}^{Q_m}\sum_{n=1}^{Q_n}\left\{\underbrace{-\left(1-\beta_i^{(1)}(V)\right)^2\left[h_{linear}(T_i)-T_i\right]^2}_{A}+\underbrace{\left\{\begin{array}{l}-2\left(1-\beta_i^{(1)}(V)\right)\left[h_{linear}(T_i)-T_i\right]\beta_i^{(2)}(V)h_{linear}\left(H_{i_v}\right)+\\ \left[\beta_i^{(2)}(V)\right]^2\left[H_{i_v}{}^2-\left[h_{linear}\left(H_{i_v}\right)\right]^2\right]\end{array}\right\}}_{B}\right\} \quad (11)$$

For the denominator in (9) to be smaller than the denominator in (8), they must be positive. This means the term B should be larger than A; it seems that this is possible if $H_{i_v}{}^2 > \left[h_{linear}\left(H_{i_v}\right)\right]^2$ and $\left(h_{linear}\left(T_i\right) - T_i\right) \approx 0$. However, if the term B is smaller than A, the SNR of the linear filtered data will be smaller than the SNR after subtraction of the haze mean. Similarly, for the median filtering, the denominator in (10) should be less than that of (8), in order for the filtered data to have larger SNR compared to before filtering. However, this is not easy to predict because separation of $\text{Median}\left(\left[1-\beta_i^{(1)}(V)\right]T_i + \beta_i^{(2)}(V)H_{i_v} + L_O\right) - \left[1-\beta_i^{(1)}(V)\right]T_i - L_O$ is not possible. Here we carry out detail analysis on Equation (9) and (10) for extreme cases, i.e. very thin haze (good visibilities) and very severe haze. When there is good visibility, the term $\beta^{(2)}(V)h_{linear}(H_V)$ is very small (Figure 4(left)), therefore its contribution in Equation (9) is very small and can be ignored. Consequently, we have:

$$\widehat{SNR} = \frac{\sum_{m=1}^{Q_m}\sum_{n=1}^{Q_n}\left\{\left[1-\beta_i^{(1)}(V)\right]T_i + L_O\right\}^2}{\sum_{m=1}^{Q_m}\sum_{n=1}^{Q_n}\left\{\left[1-\beta_i^{(1)}(V)\right]\left[h_{linear}(T_i) - T_i\right]\right\}^2} \tag{12}$$

Equation (12) indicates that the $\widehat{SNR}$ depends only on the scene itself. For average filtering, at good visibilities, the filter significantly reduces the variability within the scene. Therefore $\left[h_{linear}\left(T_i\right) - T_i\right]^2$ tends to be bigger than $\left[\beta_i^{(2)}(V)H_{i_v}\right]^2$ in Equation (7) and $\beta_i^{(2)}(V)^2\left(\overline{H}_i + H_{i_v}\right)^2$ in Equation (7); consequently, the SNR for the average filtered data tends to be lower than that of the mean subtracted data and original degraded data respectively. For Gaussian filtering using a 3 x 3 window, since the weight of the centre window is 0.9, the filtering hardly alters the original pixel, therefore $h_{linear}\left(T_i\right)$ is almost equal to T_i, consequently $\left[h_{linear}\left(T_i\right) - T_i\right]^2$ is very small and almost zero. This explains why at good visibility, the SNR of Gaussian filtered data is higher than the average filtered data. For median filtering, at good visibilities, $\beta_i^{(2)}(V)H_{i_v}$ is very small compared to $\left(1-\beta_i^{(1)}(V)\right)T_i$ and can be neglected, hence Equation (10) becomes:

$$\widehat{SNR} = \frac{\sum_{m=1}^{Q_m}\sum_{n=1}^{Q_n}\left\{\left[1-\beta_i^{(1)}(V)\right]T_i + L_O\right\}^2}{\sum_{m=1}^{Q_m}\sum_{n=1}^{Q_n}\left\{\text{Median}\left(\left[1-\beta_i^{(1)}(V)\right]T_i + L_O\right) - \left[1-\beta_i^{(1)}(V)\right]T_i - L_O\right\}^2} \tag{13}$$

Due to the non-uniformity of the signal in the data (mainly caused by variability in land features), $\left\{\text{Median}\left(\left[1-\beta_i^{(1)}(V)\right]T_i+L_O\right)-\left[1-\beta_i^{(1)}(V)\right]T_i-L_O\right\}^2$ tends to be bigger than $\left[\beta_i^{(2)}(V)H_{i_v}\right]^2$ in Equation (8) and $\left[\beta_i^{(2)}(V)\left(\overline{H_i}+H_{i_v}\right)\right]^2$ in Equation (7), consequently, the SNR of median filtered data is smaller compared to the mean subtracted data. The results for all three filters suggest that for good visibilities, it is better not to filter the data at all, because the filtering will either decrease or give about the same SNR (as for Gaussian filtering). Visibilities considered good for bands 1, 2, 3, 4, 5 and 7 are given in Table 2.

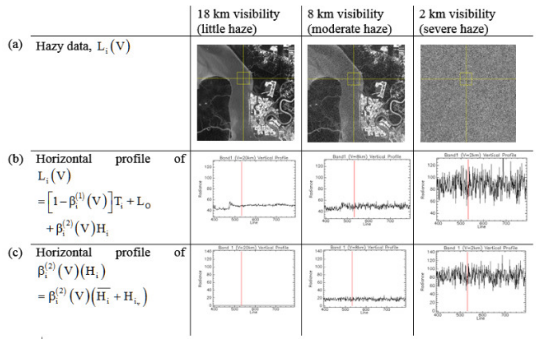

Figure 3: (a) Hazy data, (b) horizontal profile for and (c) horizontal profile for for different visibilities.

Table 2: Visibility ranges at which filtering is not required.

Band	Visibility (km)		
	Average	Median	Gaussian
1	> 8	> 8	> 10
2	> 12	> 12	> 14
3	> 10	> 10	> 12
4	> 8	> 8	> 10
5	> 8	> 8	> 12
7	> 10	> 10	> 12

Figure 3 shows (a) Hazy data, $L_i(V)$ (b) horizontal radiance profile for $L_i(V)$ and (c) horizontal radiance profile for $\beta_i^{(2)}(V)(H_i)$ associated with 18 km, 8 km and 2 km visibility in band 1. The vertical lines in (b) and (c) represent the cut along the horizontal line in (a). $\beta_i^{(2)}(V)(H_i)$ is obtained from the corresponding haze layers developed. It can be seen that at 18 km visibility, since $\beta_i^{(2)}(V)(H_i)$ is very small and almost not variable, the variation in the $L_i(V)$ is caused mainly by the scene itself, $\left[1-\beta_i^{(1)}(V)\right]T_i$ while at 2 km visibility, the variation in the $L_i(V)$ is dominated by the haze, $\beta_i^{(2)}(V)(H_i)$.For linear filtering, when the haze is very severe (i.e. short visibilities), $\beta_i^{(2)}(V)h_{\text{linear}}\left(H_{i_v}\right)$ will tend to be very variable and $\left[1-\beta_i^{(1)}(V)\right]\left[h_{\text{linear}}(T_i)-T_i\right]$ in Equation (9) is very small because of the strong signal attenuation ($\beta_i^{(1)}(V)\approx 1$) and so can be ignored; hence Equation (9) becomes:

$$\widehat{\mathrm{SNR}} = \frac{\sum_{m=1}^{Q_m}\sum_{n=1}^{Q_n}\left\{\left[1-\beta_i^{(1)}(V)\right]T_i + L_O\right\}^2}{\sum_{m=1}^{Q_m}\sum_{n=1}^{Q_n}\left[\beta_i^{(2)}(V)\, h_{\mathrm{linear}}\left(H_{i_v}\right)\right]^2} \tag{14}$$

Because of the very severe haze and the effect of averaging, here $h^2_{\mathrm{linear}}\left(H_{i_v}\right)$ tends to be smaller than $H_{i_v}{}^2$ in Equation (8) and $\left(\overline{H_i} + H_{i_v}\right)^2$ in Equation (7), therefore the average and Gaussian filtering are likely to have higher SNR than the mean subtracted data and original degraded data (Figure(b)). For median filtering, $\left[1-\beta_i^{(1)}(V)\right]T_i$ in the denominator of Equation (10) is very small compared to $\beta_i^{(2)}(V)H_{i_v}$ and so can be neglected. Hence we have:

$$\widehat{\mathrm{SNR}} = \frac{\sum_{m=1}^{Q_m}\sum_{n=1}^{Q_n}\left\{\left[1-\beta_i^{(1)}(V)\right]T_i + L_O\right\}^2}{\sum_{m=1}^{Q_m}\sum_{n=1}^{Q_n}\left[\mathrm{Median}\left(\beta_i^{(2)}(V)H_{i_v} + L_O\right) - L_O\right]^2} \tag{15}$$

Due to the very severe haze, $\left[\mathrm{Median}\left(\beta_i^{(2)}(V)H_{i_v}\right)\right]^2$ tends to be less than $\left[\beta_i^{(2)}(V)H_{i_v}\right]^2$ in Equation (8) and $\left[\beta_i^{(2)}(V)\left(\overline{H_i} + H_{i_v}\right)\right]^2$ in Equation (7). This is due to the removal of extreme values by the median filter. Consequently, the SNR of the median filtered data is likely to be higher than the mean subtracted and original degraded data. For linear filtering, for moderate haze, H_{i_v} in Equation (9) is more variable than for little haze. An optimal SNR can be achieved by keeping the denominator in Equation (9) low. In order to do so, the window size needs to be increased to effectively reduce variation in, but, at the same time, not to cause significant increase in $\left[h_{\mathrm{linear}}(T_i) - T_i\right]$. This explains why the optimal window size of the average and Gaussian filters needs to be increased as the visibility reduces (Table). The larger the window, the more effectively the variation in H_{i_v} will be reduced, but at some points, this may also cause $\left[h_{\mathrm{linear}}(T_i) - T_i\right]$ to increase, causing the SNR to drop below the optimal value. The visual effect of median filtering 12 km visibility on band 1 using 3 x 3 (left) and 21 x 21 (right) windows is shown in Figure 4. Similar SNR calculations are carried out for bands 2, 3, 4, 5 and 7.

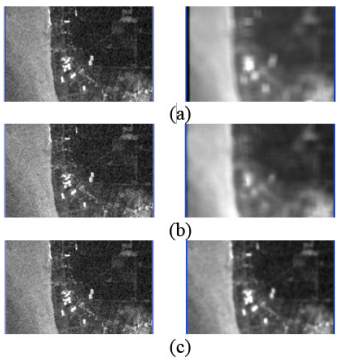

Figure 4: Visual effect of (a) average filtering, (b) median filtering and (c) Gaussian filtering with window sizes 3 x 3 (left) and 21 x 21 (right).

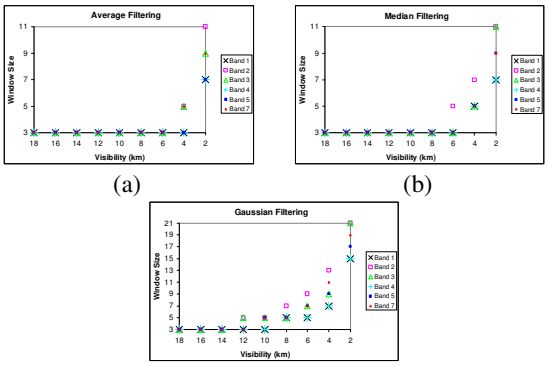

Figure 5: The optimal window size for (a) average filtering (b) median filtering and (c) Gaussian filtering for visibilities 18 to 2 km.

Figure 5((a) to (c)) show plots of window size needed to obtain the highest SNR by using average, median and Gaussian filtering respectively for visibilities 18 down to 2 km, for all bands. For average and median filtering, little variation with window size can be seen for long and moderate visibilities but larger windows are needed as visibility drops (Figure (a) and (b)). For Gaussian filtering, progressively increasing window sizes are needed with reducing visibility (Figure(c)).

4 Conclusion

In this paper, we have analysed the SNR of multispectral satellite data after restoration that involves haze weighted-mean subtraction and haze randomness filtering. In overall, the SNR for the data after Gaussian filtering, is higher than the average and median filtering. However only slight improvement of SNR is shown for good visibilities. The separation between SNR curves for the Gaussian filtered data and that of the weighted-mean subtracted data and original hazy data increases towards shorter visibilities due to the transition from smaller to larger windows, allowing the higher variation rate of $\beta^{(2)}(V)H_{i_v}$ to be reduced more effectively.

Acknowledgements. We would like to thank Universiti Teknikal Malaysia Melaka (UTeM) for funding this study under the Malaysian Ministry of Higher Education Grant (FRGS/2/2014/ICT02/FTMK/02/F00245).

References

[1] A. Ahmad, Classification Simulation of RazakSAT Satellite, *Procedia Engineering*, **53** (2013), 472 – 482.

[2] A. Ahmad and S. Quegan, Analysis of maximum likelihood classification technique on Landsat 5 TM satellite data of tropical land covers, *Proceedings of 2012 IEEE International Conference on Control System, Computing and Engineering (ICCSCE2012)*, (2012), 1 – 6. https://doi.org/10.1109/iccsce.2012.6487156

[3] A. Ahmad and S. Quegan, Comparative analysis of supervised and unsupervised classification on multispectral data, *Applied Mathematical Sciences,* **7** (2013), no. 74, 3681 – 3694. https://doi.org/10.12988/ams.2013.34214

[4] A. Ahmad, Mohd Khanapi Abdul Ghani, Sazalinsyah Razali, Haze reduction in remotely sensed data, *Applied Mathematical Sciences*, **8** (2014), no. 36, 1755 – 1762. https://doi.org/10.12988/ams.2014.4289

[5] A. Ahmad and S. Quegan, The Effects of haze on the spectral and statistical properties of land cover classification, *Applied Mathematical Sciences*, **8** (2014), no. 180, 9001 – 9013. https://doi.org/10.12988/ams.2014.411939

[6] A. Ahmad and S. Quegan, The effects of haze on the accuracy of satellite land cover classification, *Applied Mathematical Sciences*, **9** (2015), no. 49, 2433 – 2443. https://doi.org/10.12988/ams.2015.52157

[7] A. Ahmad, M. Hashim, M. N. Hashim, M. N. Ayof and A. S. Budi, The use of remote sensing and GIS to estimate Air Quality Index (AQI) Over Peninsular Malaysia, GIS development, (2006).

[8] A. Ahmad and S. Quegan, Haze modelling and simulation in remote sensing satellite data, *Applied Mathematical Sciences*, **8** (2014), no. 159, 7909 – 7921. https://doi.org/10.12988/ams.2014.49761

[9] J. R. Jensen, *Introductory Digital Image Processing: A Remote Sensing Perspective*, Pearson Prentice Hall, New Jersey, USA, 1996.

[10] M. F. Razali, A. Ahmad, O. Mohd and H. Sakidin, Quantifying haze from satellite using haze optimized transformation (HOT), *Applied Mathematical Sciences*, **9** (2015), no. 29, 1407 – 1416. https://doi.org/10.12988/ams.2015.5130

[11] M. Hashim, K. D. Kanniah, A. Ahmad, A. W. Rasib, Remote sensing of tropospheric pollutants originating from 1997 forest fire in Southeast Asia, *Asian Journal of Geoinformatics*, **4** (2004), 57 – 68.

[12] M. Story and R. Congalton, Accuracy assessment: a user's perspective, *Photogrammetric Engineering and Remote Sensing*, **52** (1986), 397 – 399.

[13] U. K. M. Hashim and A. Ahmad, The effects of training set size on the accuracy of maximum likelihood, neural network and support vector machine classification, *Science International-Lahore*, **26** (2014), no. 4, 1477 – 1481.

[14] J. R. Thomlinson, P. V. Bolstad, and W. B. Cohen, Coordinating methodologies for scaling landcover classifications from site-specific to global: steps toward validating global map products, *Remote Sensing of Environment*, **70** (1999), 16 – 28. https://doi.org/10.1016/s0034-4257(99)00055-3

Received: May 5, 2016; Published: January 24, 2017